

Organic & Biomolecular Chemistry

Accepted Manuscript



This is an *Accepted Manuscript*, which has been through the Royal Society of Chemistry peer review process and has been accepted for publication.

Accepted Manuscripts are published online shortly after acceptance, before technical editing, formatting and proof reading. Using this free service, authors can make their results available to the community, in citable form, before we publish the edited article. We will replace this *Accepted Manuscript* with the edited and formatted *Advance Article* as soon as it is available.

You can find more information about *Accepted Manuscripts* in the [Information for Authors](#).

Please note that technical editing may introduce minor changes to the text and/or graphics, which may alter content. The journal's standard [Terms & Conditions](#) and the [Ethical guidelines](#) still apply. In no event shall the Royal Society of Chemistry be held responsible for any errors or omissions in this *Accepted Manuscript* or any consequences arising from the use of any information it contains.

Targeting anti-apoptotic Bcl2 proteins with scyllatoxin-based BH3 domain mimetics

M. Margaret Harris, Zachary Coon, Najah Alqaeisoom, Brian Swords and Justin M. Holub*
Department of Chemistry and Biochemistry, Ohio University, Athens, OH 45701

**e-mail: holub@ohio.edu; Tel: +1 740-597-1228; Fax: +1 740-597-1772*

†Electronic Supplementary Information (ESI) available: Supporting figures and experimental details.

Key words: BH3 domain mimetic; induced fit; scyllatoxin; anti-apoptotic proteins; disulfide linkage.

ABSTRACT

BH3 domain mimetics based on the small protein scyllatoxin (ScTx) were designed to target the anti-apoptotic protein Bcl2 *in vitro*. Intrinsically disordered ScTx variants were found to bind Bcl2 with nanomolar affinity, indicating that an induced fit binding mechanism is required for favorable BH3:Bcl2 interaction.

Molecules that inhibit discrete protein-protein interactions (PPIs) with high precision hold great potential as therapeutic or chemical genetics agents.^{1, 2} PPIs play fundamental roles in countless metabolic pathways and are critical for maintaining proper cellular homeostasis.^{3, 4} Aberrant or dysfunctional PPIs have been implicated in a host of pathological conditions including cancer, diabetes and autoimmune disorders.⁵⁻⁷ Consequently, there is considerable interest in the design and synthesis of molecules that can target and inhibit distinct PPIs. Recent evidence has shown that many PPIs found in Nature occur between shallow, hydrophobic surface areas that are difficult to target with small molecules.⁸ Successful inhibition of these seemingly “undruggable” interactions requires molecules that are able to mimic the size and structure of protein interaction domains (PIDs).^{1, 9} Ideally, molecules designed to target and inhibit specific PPIs should display functional epitopes in orientations that mimic the architecture of native biomolecules involved in the interaction. In addition, the structure of the mimetic should be flexible enough to undergo an induced fit binding mechanism, if required.¹⁰ Functional inhibitors of PPIs must therefore strike a coordinated balance between primary sequence, spatial fixation and backbone flexibility to be effective.

The Bcl2 proteins are a family of intrinsic apoptosis regulators that control outer mitochondrial membrane permeabilization.¹¹ Anti-apoptotic Bcl2 proteins, such as Bcl-2 and Bcl-X_L, promote cell survival by sequestering pro-apoptotic Bcl2 proteins, such as Bax and Bak, on the surface of mitochondria.¹² Anti-apoptotic Bcl2 proteins have been implicated in pathogenic cell survival and have attracted interest as therapeutic targets. Structurally, pro-apoptotic Bcl2 proteins contain a semi-conserved α -helical domain (the BH3 domain) that binds to a shallow, hydrophobic cleft on the surface of anti-apoptotic Bcl2 proteins.¹³ Owing to subtle physicochemical differences between BH3 domains, anti-apoptotic Bcl2 proteins are capable of binding and neutralizing many pro-apoptotic Bcl2 members.

Inhibitors of select BH3:Bcl2 interactions have enormous potential to treat Bcl2-mediated diseases and may serve as chemical tools to investigate the differential biological functions of proteins in the Bcl2 family. Despite intense effort, however, the development of molecules that inhibit discrete BH3:Bcl2 interactions remains a significant and pressing challenge.

Over the past ten years, there have been substantial advancements in the design and synthesis of molecules that mimic α -helical PIDs (reviewed in Ref. 14). Notably, peptide α -helix mimetics have been developed as nanomolar inhibitors of the BH3:Bcl2 and p53:hDM2 interactions.^{15, 16} Helix mimetics often contain covalent linkages between amino acid side chains that lock intrinsically disordered peptides into highly stable α -helical structures. These molecules are able to display functional epitopes in patterns that are complementary to native PPI surfaces. However, covalently constraining peptide folds can reduce backbone flexibility and may preclude targeting biomolecular interactions that require induced fit binding mechanisms.^{10, 17} In an effort to determine the structural requirements for targeting anti-apoptotic Bcl2 proteins, we have grafted elements of the helical BH3 domain of Bax and Bak to the α -helix of scyllatoxin (ScTx). ScTx is a 3.4 kD protein isolated from the venom of the Israeli scorpion *L. quinquestratus* that folds into an α/β structural motif stabilized by three disulfide linkages.¹⁸ We reasoned that ScTx would be an appropriate molecule with which to evaluate the structural requirements for selective BH3:Bcl2 recognition because it contains a well-defined α -helical domain and its folded structure can be modified by the addition or removal of covalent (disulfide) linkages. Moreover, anti-apoptotic proteins in the Bcl2 family provide a well-established model system with which to test the effectiveness of helical BH3 domain mimetics.^{16, 19, 20}

It has been shown that isolated BH3 domains are intrinsically disordered in aqueous solutions at concentrations up to 25 μ M.²¹ BH3 domains will, however, form stable α -helices *in vitro* when brought into contact with anti-apoptotic Bcl2 proteins.¹⁰ Therefore, it is speculated that BH3 domains must possess an inherent helical propensity to illicit favorable BH3:Bcl2 interactions. To determine what structural elements are required for Bcl2 recognition, we synthesized three fluorescently labeled BH3 domain peptides, ^{Flu}Bax-BH3 (residues 54-74), ^{Flu}Bak-BH3 (residues 72-87) and the structural variant ^{Flu}Bak-BH3 ^{Δ APP} (Fig. 1A), and tested their ability to bind Bcl2 *in vitro*. Both ^{Flu}Bax-BH3 and ^{Flu}Bak-BH3 peptides have been used as modulators of Bcl2 activity^{22, 23} and were synthesized as positive controls. ^{Flu}Bak-BH3 ^{Δ APP} is a previously unreported structural variant of ^{Flu}Bak-BH3 that contains glycine to proline mutations at positions 75 and 82. Helix formation tends to be disfavored in peptides that contain proline within their primary sequence²⁴ and we reasoned that ^{Flu}Bak-BH3 ^{Δ APP} would be incapable of forming a helix in solution. The positions G75 and G82 were chosen because amino acid modifications at these sites are not known to significantly influence Bak:Bcl2 interactions.²⁵ For these reasons, we concluded that

$^{\text{Flu}}\text{Bak-BH3}^{\Delta\text{APP}}$ would be a useful peptide for studying whether helical propensity is required for efficient BH3:Bcl2 recognition.

All peptides were synthesized on PAL-AM resin using standard solid-phase peptide synthesis protocols (see ESI† for experimental details). To facilitate fluorescence polarization (FP) direct binding assays, each peptide was labeled at the N-terminus with 5-carboxyfluorescein. Following synthesis, the peptides were cleaved from the resin and purified to >95% by reversed-phase HPLC. Product masses were confirmed by LC/MS and peptide purities were determined by analytical HPLC (see ESI† Table S1 and Fig. S1). To evaluate the helical propensity of the BH3 domain peptides, each was dissolved to a final concentration of 10 μM in aqueous binding buffer (50 mM Tris, 100 mM NaCl, pH 8.0) and analyzed by wavelength-dependent circular dichroism (CD) spectroscopy (Fig. 1B). CD measurements were collected as mean residue ellipticity (MRE) from samples at 20 °C spanning a wavelength range from 245 to 195 nm. Under these conditions, all of the BH3 domain peptides showed CD spectra containing a slight shoulder around 220 nm and a negative maximum at 197 nm. These data suggest that $^{\text{Flu}}\text{Bax-BH3}$, $^{\text{Flu}}\text{Bak-BH3}$ and $^{\text{Flu}}\text{Bak-BH3}^{\Delta\text{APP}}$ are inherently disordered in solution, which is consistent with previous literature reports studying the solution-phase structure of isolated BH3 domain peptides.^{16,21} We next evaluated the helical propensity of $^{\text{Flu}}\text{Bax-BH3}$, $^{\text{Flu}}\text{Bak-BH3}$ and $^{\text{Flu}}\text{Bak-BH3}^{\Delta\text{APP}}$ by dissolving each peptide to a final concentration of 10 μM in binding buffer supplemented with 30% (v/v) 2,2,2-trifluoroethanol (TFE) and measuring the MRE of each peptide from 245 to 195 nm (Fig. 1C). Results from these experiments showed that both $^{\text{Flu}}\text{Bax-BH3}$ and $^{\text{Flu}}\text{Bak-BH3}$ contain double minima within their CD spectra at 220 and 204 nm, indicative of an α -helical structure. Peptide helicity was estimated using K2D2 computational methods as described previously.²⁶ $^{\text{Flu}}\text{Bax-BH3}$ and $^{\text{Flu}}\text{Bak-BH3}$ were determined to be approximately 80.7% and 50.2% helical under these conditions, respectively. The reduced helicity of $^{\text{Flu}}\text{Bak-BH3}$ compared to $^{\text{Flu}}\text{Bax-BH3}$ is likely due to the shorter sequence length of $^{\text{Flu}}\text{Bak-BH3}$ and the presence of glycine within the $^{\text{Flu}}\text{Bak-BH3}$ sequence.²⁴ These findings are consistent with previous studies evaluating the helical propensity of isolated BH3 domain peptides in aqueous buffers supplemented with TFE.^{16,21} The structural variant $^{\text{Flu}}\text{Bak-BH3}^{\Delta\text{APP}}$ showed no enhancement in helicity in the presence of TFE. Under these conditions, the CD spectrum of $^{\text{Flu}}\text{Bak-BH3}^{\Delta\text{APP}}$ showed a slight shoulder at 220 nm and negative maximum at 197 nm, indicating an intrinsically disordered structure with a helicity of approximately 11.0%. This finding is consistent with the theory that proline significantly reduces the helical propensity of peptides, even in the presence of structure inducing co-solvents.

The ability for our BH3 domain peptides to bind anti-apoptotic Bcl2 proteins was evaluated using an *in vitro* FP direct binding assay (Fig. 1D). His-tagged Bcl2 was expressed and purified from competent *E. coli* cells using standard procedures (see ESI† for experimental details). To facilitate purification, Bcl2 was expressed without its 22-residue C-terminal transmembrane domain and was designated Bcl2- ΔTM .²⁷

Direct binding assays were performed by incubating 25 nM fluorescently-labeled peptide in the presence of varying concentrations of Bcl2- Δ TM for 1 h at 25 °C (see ESI† for experimental details). Results from our direct binding assays indicated that ^{Flu}Bax-BH3 binds Bcl2- Δ TM with a K_d of 155.3 nM and ^{Flu}Bak-BH3 binds Bcl2- Δ TM with a K_d of 309.9 nM (Fig. 1E). These results are consistent with previous reports studying the binding affinity of BH3 domain peptides to Bcl2- Δ TM *in vitro*.^{16, 25} ^{Flu}Bak-BH3 ^{Δ APP} showed no significant increase in polarization under these conditions, even when incubated with up to 10 μ M Bcl2- Δ TM. Taken together, these findings indicate that intrinsically disordered BH3 domains can bind Bcl2- Δ TM under these conditions, however, helical propensity is required for favorable BH3:Bcl2 interactions. Furthermore, these results suggest that BH3:Bcl2 interactions occur through an induced fit binding mechanism.

Following confirmation that helical propensity is required for BH3 domain peptides to bind Bcl2, we used a strategy known as protein grafting^{19, 28} to develop a series of ScTx-based BH3 domain mimetics to target Bcl2- Δ TM *in vitro* (Fig. 2A). This protein grafting strategy involved identifying residues used for Bcl2 recognition by native α -helical BH3 domains and substituting them on the α -helical portion of ScTx. The rational design of our ScTx-based BH3 domain mimetics began with an analysis of the Bax-BH3:Bcl-2 and Bak-BH3:Bcl-X_L crystal structures.^{23, 25} The Bax-BH3:Bcl-2 complex shows the Bax BH3 domain (residues 58-82) bound to Bcl-2 as a six-turn α -helix with major interactions between L59, L63, I66, L70, M74 and R78 of Bax-BH3 and the BH3-binding region of Bcl-2. The Bak-BH3:Bcl-X_L complex shows the Bak BH3 domain (residues 72-87) as a three-turn α -helix with major interactions between V74, L78, I81, and I85 of Bak-BH3 and the BH3-binding region of Bcl-X_L. It has been documented that isolated Bax and Bak BH3 domains can each bind Bcl-2 and Bcl-X_L effectively, albeit with significantly different affinities.^{21, 25}

When designing the ScTx-based BH3 domain mimetics, we initially considered several possible sequence alignments between the Bax and Bak BH3 domains and the α -helical portion of ScTx. Each alignment was scored based on its ability to align BH3 residues important for Bcl2 recognition with solvent-exposed residues within the α -helix of ScTx. Sequences were also designed in a manner that aligned cysteine residues important for ScTx folding with BH3 residues that point away from the BH3:Bcl2 binding interface. This design strategy produced ScTx-based BH3 domain mimetics with α -helical regions that were near-direct sequence mimics of the Bax and Bak BH3 domains (see ESI† Fig. S2A). Importantly, the final sequences of the ScTx-based BH3 domain mimetics contained each of the hydrophobic residues required for favorable BH3:Bcl2 recognition. ScTx-Bax contained residues L59, L63, I66 and L70, and ScTx-Bak contained residues V74, L78, I81 and L/I85. In addition, each ScTx-based BH3 mimetic contained a conserved Asp residue found in all BH3 domains^{21, 23} in the proper

sequence position relative to the hydrophobic Bcl2 recognition epitope. It is important to note, however, that the three-turn α -helix of ScTx is shorter than the BH3 domains of Bax and Bak. ScTx-Bax contained 14 out of the 21 residues (66%) of the full-length Bax BH3 domain and ScTx-Bak contained 14 out of 16 (87.5%) of the full-length Bak BH3 domain. It was also noted that the BH3 domain of Bax contains a cysteine residue at position 62. Bax C62 remains in its reduced state in the native protein and is required for the H₂O₂-dependent activation of Bax in live cells.²⁹ C62 is positioned on the opposite side of the BH3 helix as the Bcl2 binding epitope and is not thought to be involved in BH3:Bcl2 recognition.²³ To reduce the possibility of misfolded protein or unwanted disulfide formation during subsequent folding reactions, ScTx-Bax was synthesized with an aminobutyric acid (Abu, B) residue in the sequence position that corresponds to Bax C62. Once the peptide sequences had been designed, we determined the backbone RMSD for each ScTx-based BH3 domain mimetic aligned with its respective native BH3 domain. PyMOL molecular modeling software was used to generate models ScTx-Bax and ScTx-Bak that were based on the solution-phase structure of wild-type ScTx (wtScTx).¹⁸ These structures were aligned with the Bax and Bak BH3 domains from the Bax-BH3:Bcl-2 and Bak-BH3:Bcl-X_L crystal structures.^{23, 25} We found that ScTx-Bax aligns with Bax-BH3 with an RMSD value of 0.738 and ScTx-Bak aligns with Bak-BH3 with an RMSD value of 0.926 (data not shown). These data suggest that the Bcl2 binding epitopes of ScTx-Bax and ScTx-Bak can adopt proper spatial orientations for favorable BH3:Bcl2 interaction.

ScTx-based BH3 mimetics were synthesized on PAL-AM resin using standard solid phase peptide synthesis procedures (see ESI† for experimental details). To facilitate subsequent FP binding studies, each ScTx-based BH3 mimetic was fluorescently labeled on its N-terminus with 5-carboxyfluorescein (Fig. 2B). The solid-phase synthesis of ^{Flu}wtScTx, ^{Flu}ScTx-Bax and ^{Flu}ScTx-Bak yielded each peptide in its fully reduced (linear) form as a major product determined by LC/MS and reversed-phase HPLC (see ESI† Table S1 and Fig. S3). Following synthesis, the reduced peptides were purified by reversed-phase HPLC and reacted under oxidative conditions³⁰ to afford fully oxidized (folded) ScTx-based BH3 mimetics (see ESI† for experimental details). Fully oxidized ScTx-based BH3 mimetics were confirmed by observing a loss in mass corresponding to six hydrogen atoms and product retention time shifts in HPLC chromatograms (see ESI† Table S1 and Fig. S3). The oxidized ScTx-based BH3 mimetics were then purified to >95% by reversed-phase HPLC to yield a single species of folded product (see ESI† Fig. S1).

Following synthesis and purification, we investigated the solution-phase structure of the oxidized, fluorescently labeled ScTx-based BH3 mimetics using wavelength-dependent CD spectroscopy (Fig. 2C). To initiate these studies, ^{Flu}wtScTx, ^{Flu}ScTx-Bax and ^{Flu}ScTx-Bak were each dissolved in binding buffer to a final concentration of 10 μ M and analyzed by CD from 245 nm to 195 nm at 20 °C. Results from these experiments revealed that each ScTx variant displayed a shoulder at 220 nm and a negative maximum at

204 nm. These data are consistent with previous results analyzing the CD spectra of ScTx-based peptides under similar conditions.³⁰ However, both ^{Flu}ScTx-Bax and ^{Flu}ScTx-Bak exhibited significantly less MRE signal compared to ^{Flu}wtScTx, indicating a more disordered structure in solution. These data suggest that ^{Flu}wtScTx is approximately 57.6% helical in aqueous buffer.²⁶ ^{Flu}ScTx-Bak and ^{Flu}ScTx-Bax were less helical under these conditions, with respective helices of 13.2% and 12.8%. The loss in helicity of ^{Flu}ScTx-Bax and ^{Flu}ScTx-Bak may be attributed to enhanced hydrophobic character or the presence of helix disrupting residues, such as Gly, contained within their α -helical regions.²⁴ To assess the thermal stability of ^{Flu}wtScTx, ^{Flu}ScTx-Bax and ^{Flu}ScTx-Bak in aqueous solution, we dissolved each peptide to a final concentration of 10 μ M in binding buffer and monitored the temperature-dependence of the MRE at 220 nm from 5 to 95 °C. None of the oxidized peptides exhibited any loss in MRE signal during these experiments, which suggests that these molecules are highly stable in aqueous solution at temperatures up to 95 °C (data not shown). Taken together, these data indicate that ^{Flu}ScTx-Bax and ^{Flu}ScTx-Bak fold similarly to ^{Flu}wtScTx in aqueous buffer (albeit with less helicity) and exhibit comparable thermal stability to ^{Flu}wtScTx at temperatures up to 95 °C.

The oxidative conditions under which synthetic ScTx-based peptides fold are well established.³⁰ However, folding conditions for ScTx-based BH3 domain mimetics have not yet been explored. Because of this, and due to the reduced helicity seen for ^{Flu}ScTx-Bax compared to ^{Flu}wtScTx, we were interested in evaluating whether native disulfide linkages were formed during the oxidative folding of ScTx-Bax (see ESI† Fig. S4A). In wtScTx, disulfide bonds are formed between cysteines C3 and C21, C8 and C26, and C12 and C28.^{18,30} To evaluate the position of the disulfide linkages in oxidized ScTx-based BH3 domain mimetics, we digested unlabeled ScTx-Bax using trypsin and evaluated the peptide fragments by LC/MS (see ESI† Fig. S4B). Trypsin was determined to be a suitable protease for mapping disulfide connectivity in ScTx-Bax because the digested proteolytic fragments result in products that contain one or two dicysteines. Trypsin digest of ScTx-Bax was conducted as described previously³⁰ and the digestion products were purified by reversed-phase HPLC (see ESI† for experimental details). The resultant product peaks were collected and analyzed by LC/MS. Observed mass values of the eluted products correlated well with peptide fragments linked through dicysteines C3 and C21, C8 and C26, or C12 and C28, indicating that ScTx-Bax contains all native disulfide bonds found in wtScTx.

We next evaluated the ability for ScTx-based BH3 mimetics to target Bcl2- Δ TM using *in vitro* FP direct binding assays (Fig. 2D). FP direct binding assays were performed by incubating 25 nM fluorescently-labeled peptide in the presence of varying concentrations of Bcl2- Δ TM for 1 h at 25 °C (see ESI† for experimental details). ^{Flu}Bak-BH3 was used as a positive control in this series of experiments and was found to bind Bcl2- Δ TM with a K_d of 215.7 nM. As expected, ^{Flu}wtScTx had no affinity for Bcl2- Δ TM, which was determined by the absence of an increase in polarization at higher concentrations

of Bcl2- Δ TM. Surprisingly, however, $^{\text{Flu}}$ ScTx-Bax and $^{\text{Flu}}$ ScTx-Bak showed no increase in polarization at higher concentrations of Bcl2- Δ TM, indicating no direct binding. K_d values for these peptides binding to Bcl2- Δ TM were not determined. We believe there are two possible reasons for this result. First, fully structured $^{\text{Flu}}$ ScTx-Bax and $^{\text{Flu}}$ ScTx-Bak show significantly less helicity in solution than $^{\text{Flu}}$ wtScTx. This more disordered, albeit rigid, structure may prevent the side chains of the hydrophobic Bcl2 binding epitope from being positioned in an optimum orientation for targeting Bcl2- Δ TM. Second, fully structured $^{\text{Flu}}$ ScTx-Bax and $^{\text{Flu}}$ ScTx-Bak show very little thermal flexibility in solution. Under the induced fit binding model of PPIs, protein folds need to be flexible to achieve optimum spatial orientations of complementary recognition elements. The rigidity of $^{\text{Flu}}$ ScTx-Bax and $^{\text{Flu}}$ ScTx-Bak may preclude the induced fit binding mechanism required for effective targeting of Bcl2- Δ TM by ScTx-based BH3 domain mimetics.

To determine whether ScTx-based BH3 domain mimetics can be engineered to target Bcl2- Δ TM through an induced fit binding mechanism, we synthesized a series of fluorescently labeled ScTx-based BH3 domain mimetics in which all structure inducing cysteines were replaced with Abu (Fig. 3A). These ScTx-based proteins were designated $^{\text{Flu}}$ wtScTx $^{\Delta\Delta\Delta}$, $^{\text{Flu}}$ ScTx-Bax $^{\Delta\Delta\Delta}$ and $^{\text{Flu}}$ ScTx-Bak $^{\Delta\Delta\Delta}$ to indicate loss of three disulfide linkages. Abu has been used to replace structural cysteines of ScTx in studies evaluating the influence of disulfide linkages on the biological activity of wtScTx.³⁰ Except for the Cys to Abu mutations, each ScTx-based structural variant was identical in sequence to their structured counterpart (see ESI† Fig. S2B). All ScTx-based structural variants were synthesized on PAL-AM resin using solid-phase synthesis procedures and purified to >95% by reversed-phase HPLC (see ESI† for experimental details). To facilitate subsequent FP binding studies, each ScTx-based structural variant was fluorescently labeled on its N-terminus with 5-carboxyfluorescein. Product masses were confirmed by LC/MS and peptide purities were determined by analytical HPLC (see ESI† Table S1 and Fig. S1). No oxidation (folding) reactions were performed on the structural variants.

We speculated that, in the absence of structure-inducing cysteines, $^{\text{Flu}}$ wtScTx $^{\Delta\Delta\Delta}$, $^{\text{Flu}}$ ScTx-Bax $^{\Delta\Delta\Delta}$ and $^{\text{Flu}}$ ScTx-Bak $^{\Delta\Delta\Delta}$ would be intrinsically disordered in aqueous buffer. To evaluate the solution-phase structure of these peptides, we dissolved each to a final concentration of 10 μ M in binding buffer and analyzed the samples using wavelength-dependent CD spectroscopy (Fig. 3B). CD scans were performed from 250 nm to 190 nm at 20 °C. Under these conditions, each ScTx-based structural variant showed a slight shoulder at 220 nm and a negative maximum near 195 nm, indicating they adopt inherently disordered structures in solution. To determine whether ScTx-based structural variants have the propensity to fold in aqueous buffer, we dissolved each peptide to a final concentration of 10 μ M in binding buffer supplemented with 30% (v/v) TFE and analyzed the samples by CD spectroscopy (Fig.

3C). Wavelength scans were performed on each sample from 250 nm to 190 nm at 20 °C. Interestingly, each ScTx-based structural variant showed spectra indicative of folded ScTx-based peptides, with a shoulder at 220 nm, a negative maximum at 204 nm and a positive maximum at 193 nm. $^{Flu}wtScTx^{\Delta\Delta\Delta}$ and $^{Flu}ScTx-Bak^{\Delta\Delta\Delta}$ were similarly helical with approximate helicities of 67.4% and 67.8% respectively.²⁶ $^{Flu}ScTx-Bax^{\Delta\Delta\Delta}$ was determined to be slightly less helical at approximately 62.6%. The reduced helicity for $^{Flu}ScTx-Bax^{\Delta\Delta\Delta}$ is likely due to a relatively high density of cationic charges within its α -helical region and a shorter helix length compared to $^{Flu}wtScTx^{\Delta\Delta\Delta}$ and $^{Flu}ScTx-Bak^{\Delta\Delta\Delta}$. These data suggest that ScTx-based structural variants undergo a significant transition from intrinsically disordered to predominantly helical in the presence of structure-inducing co-solvents. Furthermore, these results indicate that structural variants of ScTx-based proteins have the propensity to fold into structures that are reminiscent of fully oxidized (folded) wtScTx.

We theorized that intrinsically disordered ScTx-based BH3 domain mimetics that demonstrate a propensity to fold in aqueous buffer would be better suited to bind Bcl2 proteins through an induced fit binding mechanism than their structured counterparts. To test this hypothesis, we evaluated the ability for the intrinsically disordered ScTx-based BH3 domain mimetics to bind Bcl2- Δ TM using an *in vitro* FP direct binding assay (Fig. 3D). FP direct binding assays were performed by incubating 25 nM fluorescently-labeled peptide in the presence of varying concentrations of Bcl2- Δ TM for 1 h at 25 °C (see ESI† for experimental details). $^{Flu}wtScTx^{\Delta\Delta\Delta}$ did not bind Bcl2- Δ TM in this series of experiments, as was determined by an absence of increased polarization at higher concentrations of Bcl2- Δ TM. Notably, $^{Flu}ScTx-Bax^{\Delta\Delta\Delta}$ and $^{Flu}ScTx-Bak^{\Delta\Delta\Delta}$ were found to bind Bcl2- Δ TM with mid to high nanomolar affinity (Fig. 3E). $^{Flu}ScTx-Bak^{\Delta\Delta\Delta}$ binds Bcl2- Δ TM with a K_d of 826.5 nM and $^{Flu}ScTx-Bax^{\Delta\Delta\Delta}$ bound Bcl2- Δ TM with a K_d of 268.9 nM. These results indicate that, despite their lack of structure, intrinsically disordered ScTx-based BH3 domain mimetics can be engineered to bind to Bcl2- Δ TM *in vitro*. Moreover, these results support the induced fit binding model of BH3:Bcl2 interactions and suggest that rigid peptide structures may not be optimum for targeting Bcl2 proteins. Perhaps more significant is the degree of selectivity with which the inherently disordered ScTx-based BH3 domain mimetics bind Bcl2- Δ TM *in vitro*. $^{Flu}ScTx-Bax^{\Delta\Delta\Delta}$ was found to bind Bcl2- Δ TM with nearly three times greater affinity than $^{Flu}ScTx-Bak^{\Delta\Delta\Delta}$. Given the physicochemical and structural similarities between the Bcl2-binding epitopes of $^{Flu}ScTx-Bax^{\Delta\Delta\Delta}$ and $^{Flu}ScTx-Bak^{\Delta\Delta\Delta}$ (see ESI† Fig. S2A), selectivity for Bcl2- Δ TM is likely influenced by other residues within their primary sequences. For example, $^{Flu}ScTx-Bax^{\Delta\Delta\Delta}$ contains a Lys at position 11, which corresponds to K64 of the native Bax-BH3 domain. Upon favorable Bax-BH3:Bcl2 interaction, this cationic residue is thought to form a stable hydrogen bond with D140 of Bcl2.²³ Contrarily, $^{Flu}ScTx-Bak^{\Delta\Delta\Delta}$ contains an Ala in the same position, which is not expected to interact with D140 of Bcl2 as

favorably. It should also be noted that the difference in selectivity for Bcl2- Δ TM is greater between ScTx-based BH3 domain mimetics than between native BH3 domains (compare Figs. 1E and 3E). This result may support the use of ScTx-based BH3 domain mimetics as highly selective therapeutics or chemical genetics agents to modulate discrete BH3:Bcl2 interactions.

CONCLUSIONS

In summary, we have developed a new class of BH3 domain mimetic based on the small protein scyllatoxin that targets anti-apoptotic Bcl2 proteins *in vitro*. By screening a library of structural variants, we determined that fully oxidized (folded) ScTx-based BH3 domain mimetics do not bind Bcl2- Δ TM, while intrinsically disordered constructs target Bcl2- Δ TM with nanomolar affinity. These results suggest that a certain degree of backbone flexibility is required for favorable BH3:Bcl2 interactions. Furthermore, we have shown that ScTx-based Bax mimetics bind Bcl2- Δ TM with nearly three times greater affinity than ScTx-Bak variants, indicating that discrete BH3 domain sequences are capable of imparting selectivity to this class of BH3 domain mimetic. In a more generalized sense, we believe that ScTx-based PID mimetics have the potential to become valuable tools in the laboratory for studying the interplay between primary sequence, spatial fixation, and backbone flexibility required to successfully target discrete PPIs. Research is currently underway in our laboratory to determine what influence disulfide connectivity has on Bcl2 recognition by ScTx-based BH3 domain mimetics.

ACKNOWLEDGEMENTS

This work was supported by the Department of Chemistry and Biochemistry, the College of Arts and Sciences and the Vice President for Research at Ohio University. The authors would like to thank Drs. Hao Chen, Michael Held, Jennifer Hines and Marcia Kieliszewski for technical support. J.M.H. would like to dedicate this manuscript to the memory of Professor Bruce S. Burnham of Rider University.

REFERENCES

1. V. Azzarito, K. Long, N. S. Murphy and A. J. Wilson, *Nat Chem*, 2013, **5**, 161-173.
2. S. R. Nirantar, X. Li, J. W. Siau and F. J. Ghadessy, *Biosens Bioelectron*, 2014, **56**, 250-257.
3. R. M. Kaake, X. Wang and L. Huang, *Mol Cell Proteomics*, 2010, **9**, 1650-1665.
4. M. Taipale, G. Tucker, J. Peng, I. Krykbaeva, Z. Y. Lin, B. Larsen, H. Choi, B. Berger, A. C. Gingras and S. Lindquist, *Cell*, 2014, **158**, 434-448.
5. Y. J. Huang, D. Hang, L. J. Lu, L. Tong, M. B. Gerstein and G. T. Montelione, *Mol Cell Proteomics*, 2008, **7**, 2048-2060.
6. T. Tuller, S. Atar, E. Ruppin, M. Gurevich and A. Achiron, *Genes Immun*, 2013, **14**, 67-82.
7. J. Han, M. Zhang, S. Froese, F. F. Dai, M. Robitaille, A. Bhattacharjee, X. Huang, W. Jia, S. Angers, M. B. Wheeler and L. Wei, *PLoS One*, 2015, **10**, e0129226.
8. N. Tsomaia, *Eur J Med Chem*, 2015, **94**, 459-470.
9. L. K. Tsou, Y. Cheng and Y. C. Cheng, *Curr Opin Pharmacol*, 2012, **12**, 403-407.
10. J. M. Rogers, A. Steward and J. Clarke, *J Am Chem Soc*, 2013, **135**, 1415-1422.
11. B. Leibowitz and J. Yu, *Cancer Biol Ther*, 2010, **9**, 417-422.
12. P. E. Czabotar, G. Lessene, A. Strasser and J. M. Adams, *Nat Rev Mol Cell Biol*, 2014, **15**, 49-63.
13. A. M. Petros, E. T. Olejniczak and S. W. Fesik, *Biochim Biophys Acta*, 2004, **1644**, 83-94.
14. C. Billard, *Mol Cancer Ther*, 2013, **12**, 1691-1700.
15. F. Bernal, A. F. Tyler, S. J. Korsmeyer, L. D. Walensky and G. L. Verdine, *J Am Chem Soc*, 2007, **129**, 2456-2457.
16. D. Wang, W. Liao and P. S. Arora, *Angew Chem Int Ed Engl*, 2005, **44**, 6525-6529.
17. S. Gianni, J. Dogan and P. Jemth, *Biophys Chem*, 2014, **189**, 33-39.
18. J. C. Martins, F. J. Van de Ven and F. A. Borremans, *J Mol Biol*, 1995, **253**, 590-603.
19. J. W. Chin and A. Schepartz, *Angew Chem Int Ed Engl*, 2001, **40**, 3806-3809.
20. L. D. Walensky, A. L. Kung, I. Escher, T. J. Malia, S. Barbuto, R. D. Wright, G. Wagner, G. L. Verdine and S. J. Korsmeyer, *Science*, 2004, **305**, 1466-1470.
21. L. Chen, S. N. Willis, A. Wei, B. J. Smith, J. I. Fletcher, M. G. Hinds, P. M. Colman, C. L. Day, J. M. Adams and D. C. Huang, *Mol Cell*, 2005, **17**, 393-403.
22. S. Dutta, S. Gulla, T. S. Chen, E. Fire, R. A. Grant and A. E. Keating, *J Mol Biol*, 2010, **398**, 747-762.
23. B. Ku, C. Liang, J. U. Jung and B. H. Oh, *Cell Res*, 2011, **21**, 627-641.
24. M. Alias, S. Ayuso-Tejedor, J. Fernandez-Recio, C. Cativiela and J. Sancho, *Org Biomol Chem*, 2010, **8**, 788-792.
25. M. Sattler, H. Liang, D. Nettessheim, R. P. Meadows, J. E. Harlan, M. Eberstadt, H. S. Yoon, S. B. Shuker, B. S. Chang, A. J. Minn, C. B. Thompson and S. W. Fesik, *Science*, 1997, **275**, 983-986.
26. C. Perez-Iratxeta and M. A. Andrade-Navarro, *BMC Struct Biol*, 2008, **8**, 25.
27. M. L. Stewart, E. Fire, A. E. Keating and L. D. Walensky, *Nat Chem Biol*, 2010, **6**, 595-601.
28. J. A. Kritzer, R. Zutshi, M. Cheah, F. A. Ran, R. Webman, T. M. Wongjirad and A. Schepartz, *Chembiochem*, 2006, **7**, 29-31.
29. C. Nie, C. Tian, L. Zhao, P. X. Petit, M. Mehrpour and Q. Chen, *J Biol Chem*, 2008, **283**, 15359-15369.
30. Q. Zhu, S. Liang, L. Martin, S. Gasparini, A. Menez and C. Vita, *Biochemistry*, 2002, **41**, 11488-11494.

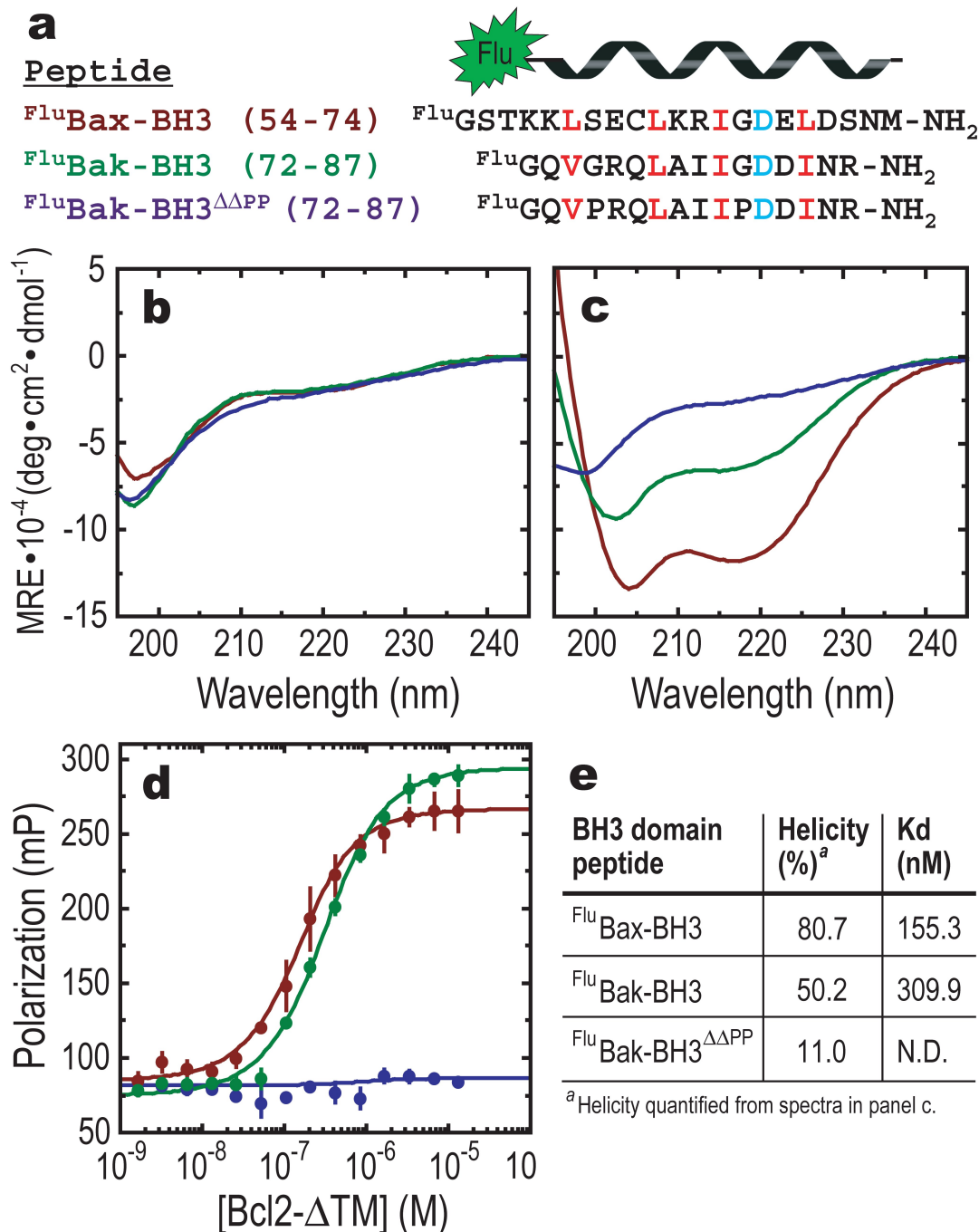


Fig. 1 A. Sequence alignment of BH3 domain peptides used to target Bcl2- Δ TM *in vitro*. Key α -helical residues required for Bcl2- Δ TM recognition are colored red; conserved BH3 domain aspartic acid is cyan. B. CD spectra of BH3 domain peptides (10 μ M) in binding buffer. See panel A for color-coded legend. C. CD spectra of BH3 domain peptides (10 μ M) in binding buffer supplemented with 30% (v/v) TFE. D. *In vitro* direct binding of BH3 domain peptides to Bcl2- Δ TM in binding buffer measured by fluorescence polarization. Data points represent an average of three independent experiments; error bars are standard deviation. E. Data from CD and direct binding experiments. N.D., not determined.

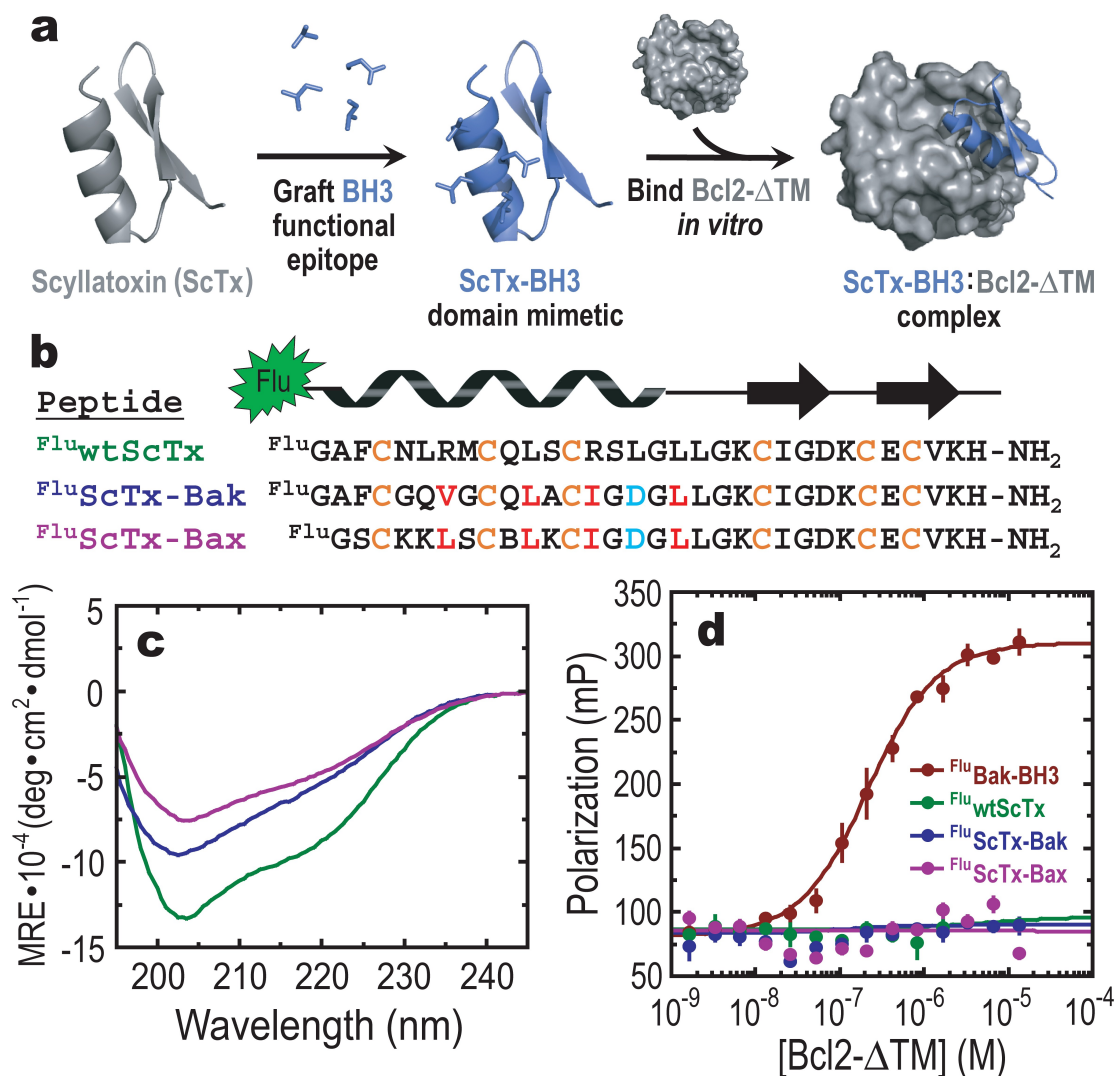


Fig. 2 A. Strategy for targeting Bcl2- Δ TM with ScTx-based BH3 domain mimetics. B. Sequence alignment of ScTx-based BH3 domain mimetics. Key α -helical residues required for Bcl2- Δ TM recognition are colored red; cysteines that contribute to ScTx folding are orange; conserved BH3 domain aspartic acid is cyan. C. CD spectra of ScTx-based BH3 domain mimetics (10 μ M) in binding buffer. See panel B for color-coded legend. D. Direct binding of Bak-BH3 peptide and ScTx-based BH3 domain mimetics to Bcl2- Δ TM in binding buffer measured by fluorescence polarization. Data points represent an average of three independent experiments; error bars are standard deviation.

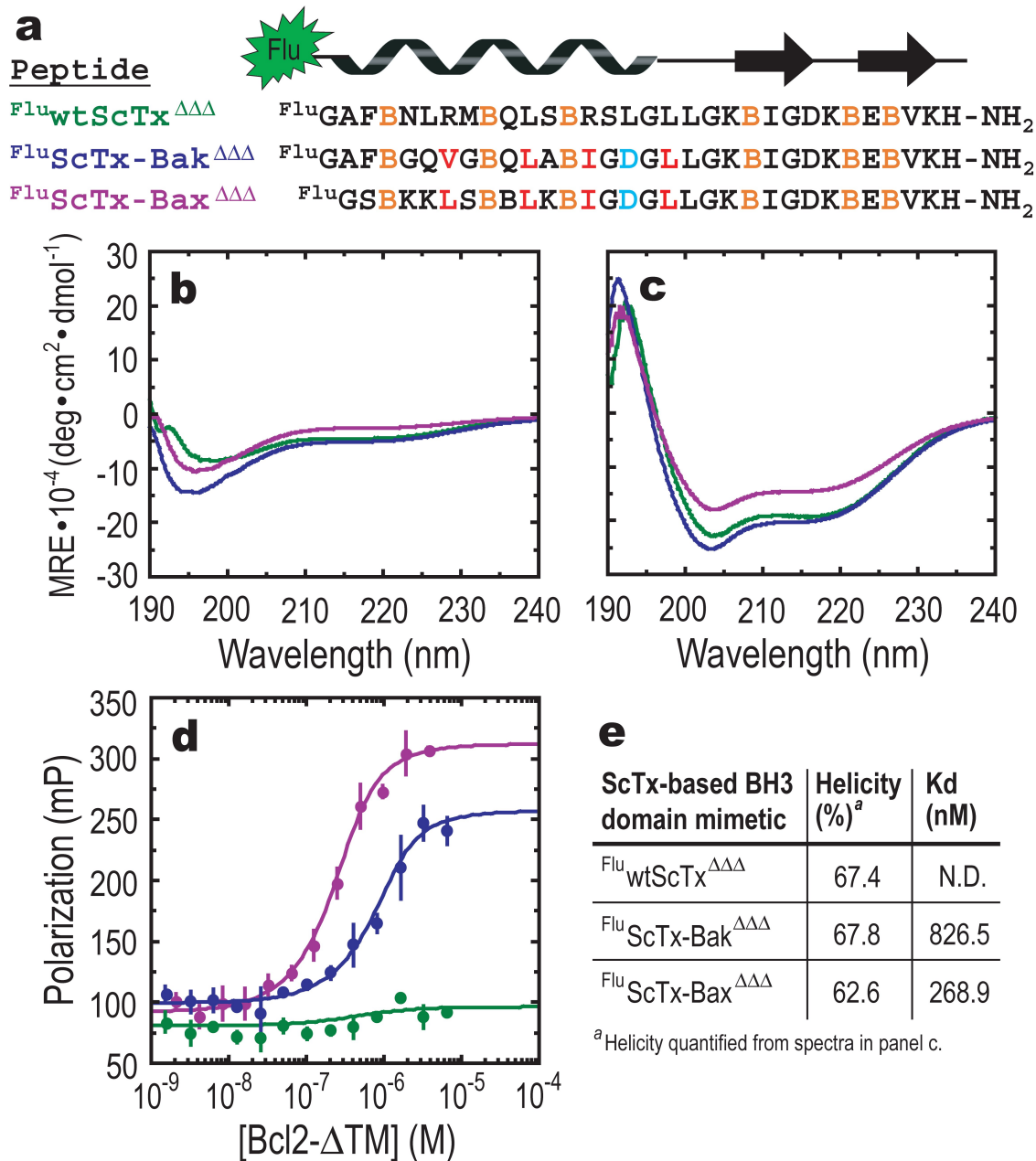


Fig. 3 A. Sequence alignment of intrinsically disordered ScTx-based BH3 domain mimetics. Key α -helical residues required for Bcl-2 recognition are colored red; aminobutyric acid residues are orange; conserved BH3 aspartic acid is cyan. B. CD spectra of intrinsically disordered ScTx-based BH3 domain mimetics (10 μ M) in binding buffer. See panel A for color-coded legend. C. CD spectra of intrinsically disordered ScTx-based BH3 domain mimetics (10 μ M) in binding buffer supplemented with 30% (v/v) TFE. D. Direct binding of intrinsically disordered ScTx-based BH3 domain mimetics to Bcl2- Δ TM in binding buffer measured by fluorescence polarization. Data points represent an average of three independent experiments; error bars are standard deviation. E. Data from CD and direct binding experiments. N.D., not determined.